Supplementary Information

Highly reusable nanoporous silver sheet for sensitive SERS detection of pesticides

Huanyu Chi[a, b], Congcheng Wang[c] , Zhien Wang[b], Hongni Zhu[a,b], Vince St. Dollente Mesias[b], Xin Dai[b], Qing Chen[a,b,c], Wei Liu[d], and Jinqing Huang[*,a,b]

[a]HKUST-Shenzhen Research Institute, No. 9 Yuexing first RD, Hi-tech Park, Nanshan, Shenzhen 518057, China

[b]Department of Chemistry, [c]Department of Mechanical and Aerospace Engineering, The Hong Kong University of Science and Technology, Clear Water Bay, Kowloon, Hong Kong, China.

[d]Department of Chemistry, The University of Hong Kong, Pokfulam Road, Hong Kong, China

*Corresponding Author: Jinqing Huang

Email: jqhuang@ust.hk

1. Faraday's Electrolysis Equation in the Synthesis of the NPAg sheets.

Faraday's law was used to estimate the required charge (Q) to produce a certain depth of the nanoporous layer (d). d is related to Q as in

$$Q = \frac{nFm}{M} = \frac{2nF\rho Ad}{M}$$

where F is the Faraday constant, 96485 C mol^{-1}, n the number of electrons transferred during the oxidation of Ag to AgCl (one), ρ the density of AgCl, A the area of the sheet, and the factor of two from the fact that both sides of the sheet are later turned to NPAg. We use the density of AgCl here because very little volume change is observed in the RID of AgCl. If we synthesize a 1.7 cm X 1.2 cm NPAg sheet with a porous depth of 300 nm, the amount of charge required would be

$$m = \rho \cdot V = 5.56\ g \cdot cm^{-3} \times 300\ nm \times 1.7\ cm\ \times\ 1.2\ cm \times 2 = 0.34\ mg$$

Thus, the amount of electricity was obtained,

$$Q = \frac{1 \times 96485\ C/mole \times 5.56\ g \cdot cm^{-3} \times 300\ nm \times 1.7\ cm\ \times\ 1.2\ cm \times 2}{143.5\ g/mole} = 0.23\ C$$

2. SERS Measurement with Iodide-Modified Ag NPs (Ag NPs@KI).

Protocol referred to Ren Bin's work[1], and some changes were made. 50 mL of a 1 mM silver nitrate aqueous solution was heated to boiling. Then 1 mL of a 1% (w/v) trisodium citrate solution was fast added into solution. The mixture was kept boiling for 1 h, under constant stirring at 350 rpm, and then cooling down at room temperature. The resultant colloidal mixture was of dark gray color. 1 mL colloid was centrifuged (5000 rpm, 10min) and concentrated to 30 μL. The 30 μL solution was mixed with 30 μL 1 mM potassium iodide aqueous solution and incubated at room temperature for 20 min. Ag NPs@KI colloid was obtained. Ag NPs@KI were mixed with sample solution at room temperature in glass well. Several drops of 0.1 M magnesium sulfate solution were quickly added as aggregation agent, resulting dark brown color immediately.

3. SERS Measurement with Spermine-Modified Ag NPs (Ag NPs@sp).

Protocol referred to Ramon A. Alvarez-Puebla's work[2]. 20 μL of a 0.5 M silver nitrate aqueous solution and 7 μL of 0.1 M spermine tetrahydrochloride solution were subsequently mixed with 10 mL of Milli-Q ultrapure water. After 20 min of stirring, 250 μL of a 0.01 M freshly prepared sodium borohydride solution was rapidly injected into the mixture. Vials employed for particle preparation and storage were previously coated with polyethyleneimine (PEI) to prevent the adhesion of positively charged nanoparticles to glass surfaces. Silver colloids were left overnight to equilibrate. Ag NPs@sp colloid was obtained. Ag NPs@sp were taken in the upper transparent liquid and mixed with sample solution at room temperature in glass well. No aggregation agent was needed.

4. Enhancement Factor Calculation

The enhancement factor of the NPAg sheets was calculated according to the following equation,[3–5]

$$EF = \frac{I_{SERS}}{N_{SERS}} / \frac{I_{bulk}}{N_{bulk}}$$

where I_{SERS} and I_{bulk} represent the intensity of characteristic peak in SERS spectrum and normal Raman spectrum, N_{SERS} and N_{bulk} represent the number of molecules in the scattering volume on the SERS substrate and in bulk solution, respectively. I_{SERS} and I_{bulk} were directly obtained from the spectra of analytes, with the characteristic peak at 343 cm^{-1} of lindane. N_{SERS} and N_{bulk} needed more calculation and assumption.

Assuming that porous structures were full of analyte solution and all molecules in that volume were adsorbed to the metal surface, then N_{SERS} was estimated as follows,

$$N_{SERS} = \frac{1}{2} \times \frac{S_{laser}}{S_{sheet}} \times CVN_A$$

where C is the concentration of lindane solution (300 nM), V is the volume of porous structures, 2 mm × 2 mm area with 300 nm thickness on both sides, and N_A is Avogadro's constant, 6.02×10^{23} mol^{-1}.

Normal Raman spectrum was obtained measuring the stock solution in an 8 mm × 6 mm glass well. Assuming that the laser passed through the very thin liquid layer, N_{bulk} can be estimated as follows,

$$N_{bulk} = \frac{S_{laser}}{S_{well}} \cdot CVN_A$$

where C is the concentration of lindane solution (10 mM), V is the volume of solution, 20 μL, and N_A is Avogadro's constant, 6.02×10^{23} mol^{-1}.

Therefore, EF was calculated according to the expression. EF of lindane in this study is 2.44×10^{9}.

5. Limit of Detection (LOD) Calculation

As shown in Figure 3A, the minimum detectable concentration by experiments [6,7] of lindane aqueous solution is at around 3×10^{-7} M, with molecular weight 291 g mol^{-1}. Hence, the limit of detection can be also expressed by mass concentration as,

$$c = C \times M = 3 \times 10^{-7} \times 291\ g \cdot L^{-1} = 8.73 \times 10^{-2}\ mg \cdot L^{-1} = 87.3\ ppb$$

Also, theoretical LOD could be estimated through the following steps, which are widely accepted in SERS quantitative analysis.[8–10] Noise signals of blank background were measured to value the standard deviation, σ. Then the minimum detectable signal is taken as three times the standard deviation (3σ). Then LOD is calculated by interpolating from the linear curves the minimum concentration that results in a signal larger than the 3σ level. In this study, estimated LOD of lindane was calculated as 30 nM (8.73 ppb).

Surface Morphology

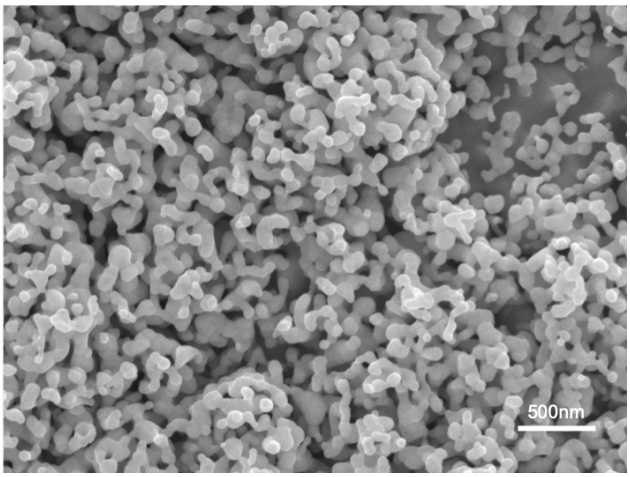

Figure S1. SEM Photo of NPAg sheets with 30,000x (scale bar 500 nm)

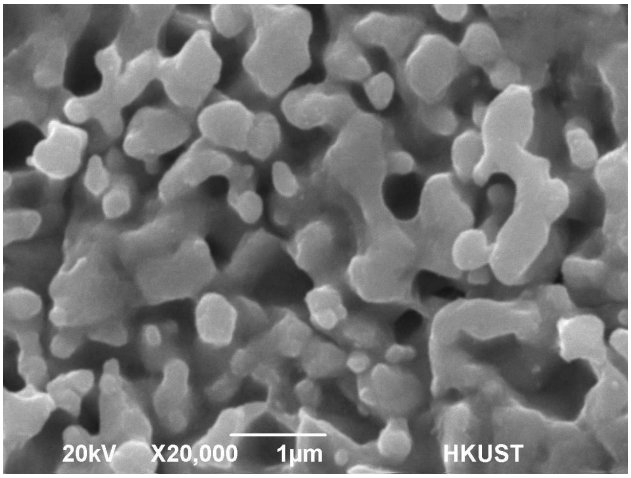

Figure S2. SEM Photo of NPAg sheets after using more than 20 times with 20,000x (scale bar 1 μm)

Chemical Stability

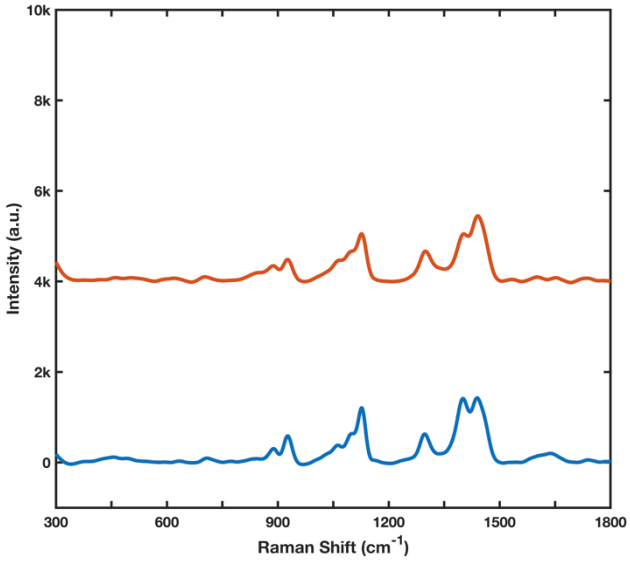

Figure S3. Normal Raman spectra of NPAg sheets before (blue) and after a month (red).

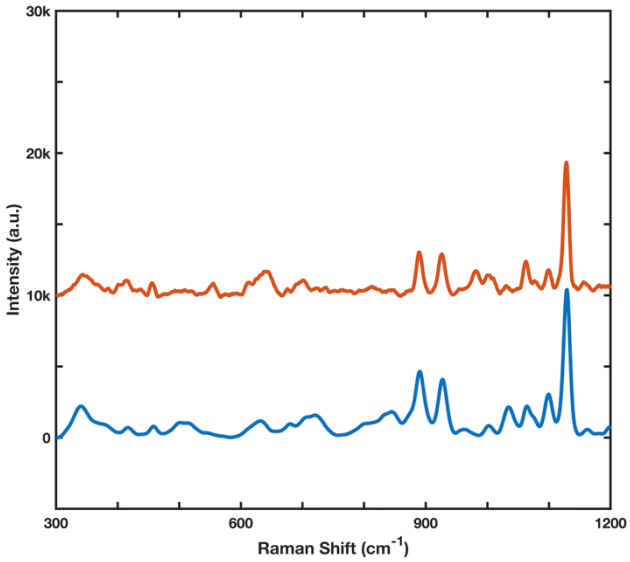

Figure S4. SERS Spectra of lindane before (blue) and after a month (red).

Detection of Rhodamine B

Table S1. Peak assignment for SERS spectrum of Rhodamine B[11]

Raman Shift (cm^{-1})	Tentative Assignment
1644	ring stretching, C-H bending
1596	ring stretching, N-H bending
1507	ring stretching, C-N stretching, C-H bending, N-H bending
1359	ring stretching, C-H bending
1195	ring deformation, C-H bending, N-H bending
622	ring deformation

Normal Raman Spectrum of Lindane

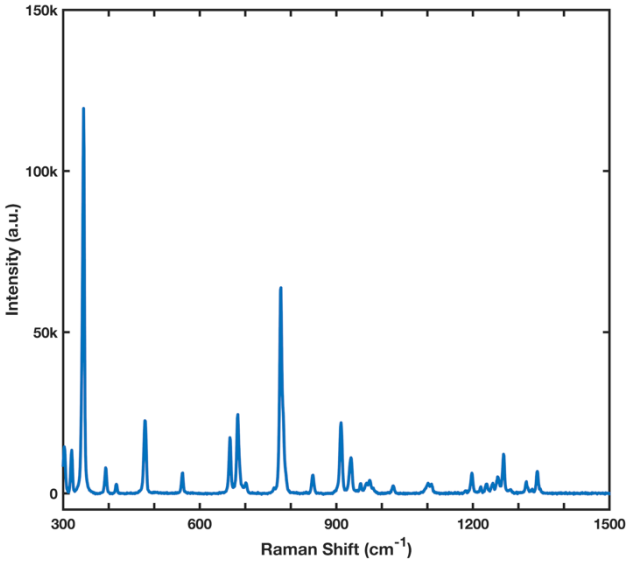

Figure S5. Raman spectrum of solid lindane.

Comparison with Silver Nanoparticles

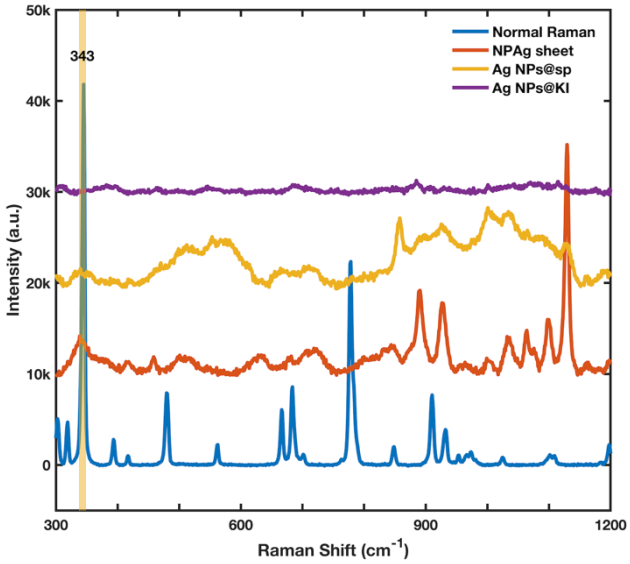

Figure S6. Raman spectrum (blue) and SERS spectra of 1 μM lindane solution on NPAg sheet (red), Ag NPs@sp (yellow), Ag NPs@KI (purple).

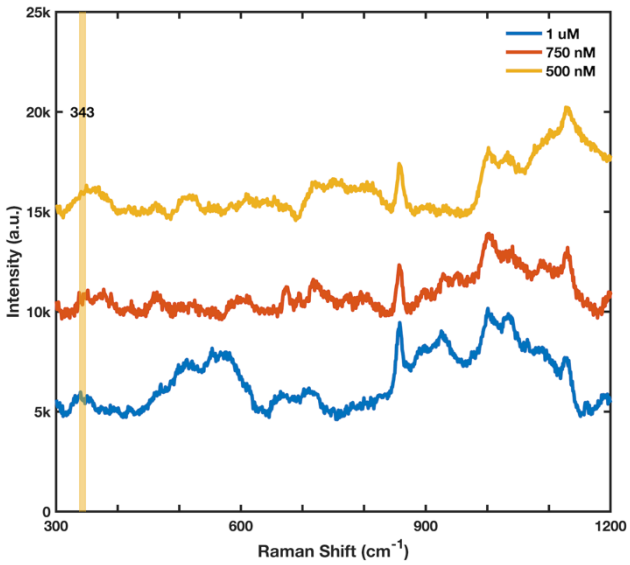

Figure S7. SERS spectra of lindane solution at different concentrations (top to bottom, from 500 nM to 1 μM) obtained from silver nanoparticles coated with spermine.

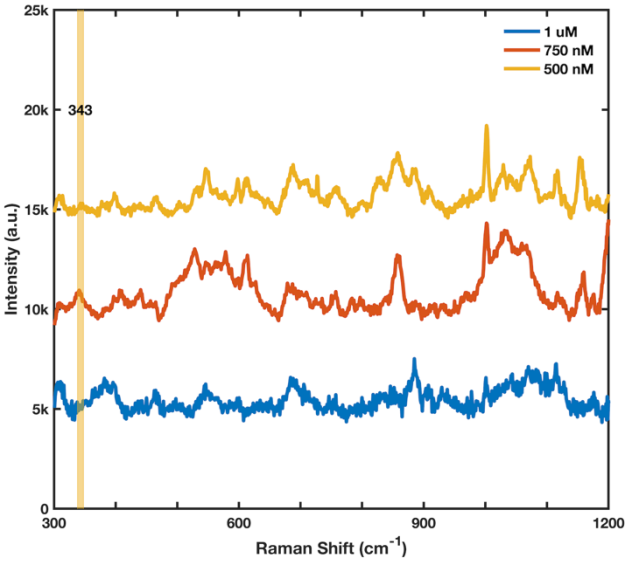

Figure S8. SERS spectra of lindane solution at different concentrations (top to bottom, from 500 nM to 1 μM) with silver nanoparticles coated with potassium iodide.

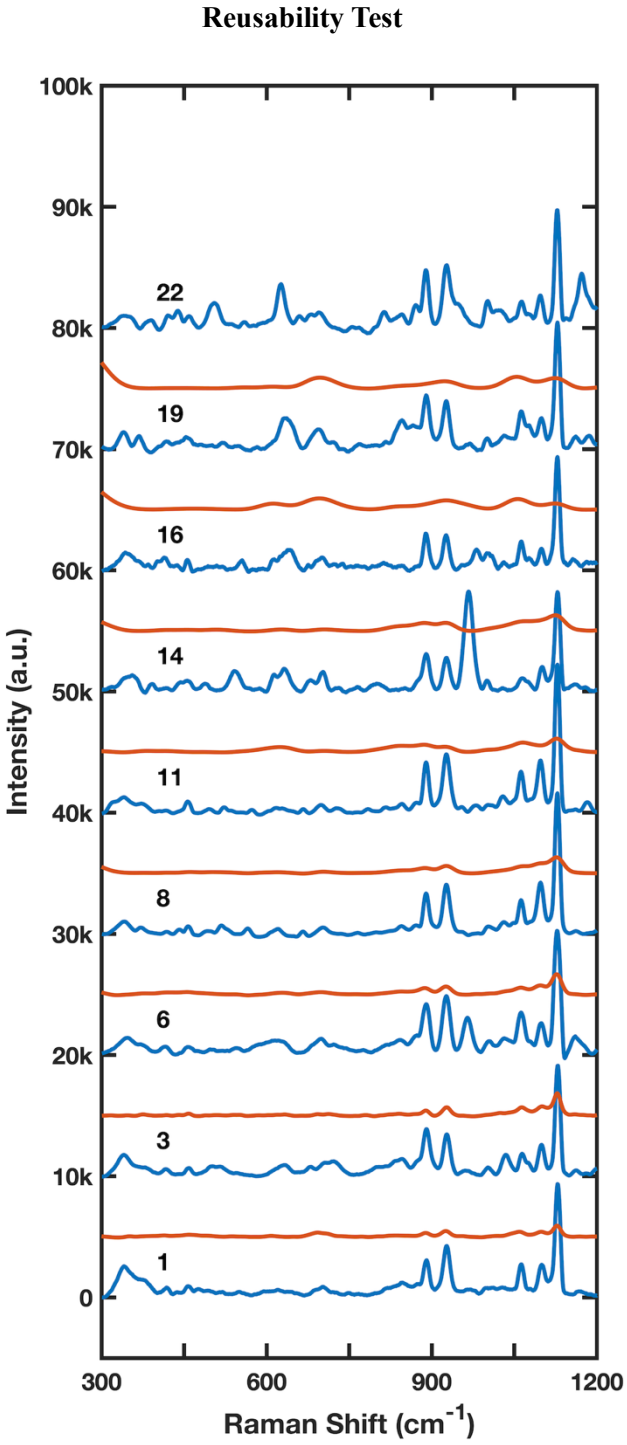

Figure S9. Reusability test SERS spectra of NPAg sheets for SERS spectral detection of 1μM lindane solution (blue) and blank baseline after ultrasonic wash (red) up to 22 cycles.

Detection of Dichlorodiphenyltrichloroethane (DDT)

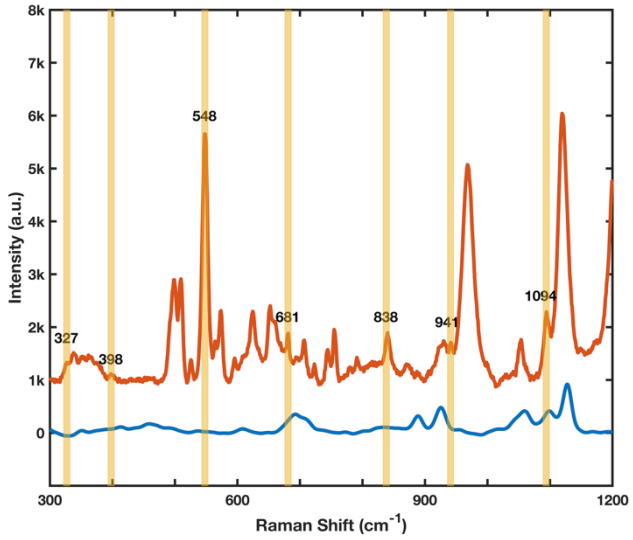

Figure S10. SERS spectrum of DDT solution (red) and background spectrum of the NPAg sheet (blue).

Table S2. Peak assignment for SERS spectrum of DDT[12,13]

Raman Shift (cm^{-1})	**Tentative Assignment**
1094	ring breath, C-H bending
941	ring formation
838	C-H twisting
681, 548	C-Cl stretching
398	C-Cl symmetrical stretching
327	C-Cl anti-symmetrical stretching

Reference

1 L. J. Xu, C. Zong, X. S. Zheng, P. Hu, J. M. Feng and B. Ren, *Anal. Chem.*, 2014, **86**, 2238–2245.

2 L. Guerrini, Ž. Krpetić, D. Van Lierop, R. A. Alvarez-Puebla and D. Graham, *Angew. Chemie Int. Ed.*, 2015, **54**, 1144–1148.

3 S. E. J. Bell and N. M. S. Sirimuthu, *Chem. Soc. Rev.*, 2008, **37**, 1012–1024.

4 E. C. Le Ru, E. Blackie, M. Meyer and P. G. Etchegoint, *J. Phys. Chem. C*, 2007, **111**, 13794–13803.

5 S. Akil-Jradi, S. Jradi, J. Plain, P. M. Adam, J. L. Bijeon, P. Royer and R. Bachelot, *RSC Adv.*, 2012, **2**, 7837–7842.

6 D. Chen, X. Zhu, J. Huang, G. Wang, Y. Zhao, F. Chen, J. Wei, Z. Song and Y. Zhao, *Anal. Chem.*, 2018, **90**, 9048–9054.

7 S. Liu, J. Yu, T. Wang and F. Li, *J. Mater. Sci.*, 2017, **52**, 13748–13763.

8 S. H. Yazdi and I. M. White, *Anal. Chem.*, 2012, **84**, 7992–7998.

9 W. Wei, Y. Du, L. Zhang, Y. Yang and Y. Gao, *J. Mater. Chem. C*, 2018, **6**, 8793–8803.

10 D. M. Kuncicky, B. G. Prevo and O. D. Velev, *J. Mater. Chem.*, 2006, **16**, 1207–1211.

11 A. M. Michaels, M. Nirmal and L. E. Brus, *J. Am. Chem. Soc.*, 1999, **121**, 9932–9939.

12 A. Mariño-Lopez, A. Sousa-Castillo, M. Blanco-Formoso, L. N. Furini, L. Rodríguez-Lorenzo, N. Pazos-Perez, L. Guerrini, M. Pérez-Lorenzo, M. A. Correa-Duarte and R. A. Alvarez-Puebla, *ChemNanoMat*, 2019, **5**, 46–50.

13 P. Aldeanueva-Potel, E. Faoucher, R. A. Alvarez-Puebla, L. M. Liz-Marzán and M. Brust, *Anal. Chem.*, 2009, **81**, 9233–9238.